VOL. 9, NO. 8, AUGUST 2014 ISSN 1819-6608
ARPN Journal of Engineering and Applied Sciences


www.arpnjournals.com

EFFECT OF SENSOR DEBONDING ON LAMB WAVE PROPAGATION IN PLATE STRUCTURE

C. N. Sathyanarayana[1, 2], U. Ashwin[1, 2] and S. Raja[1]
[1]Dynamics and Adaptive Structures Group, Structural Technologies Division, CSIR-National Aerospace Laboratories, Bangalore, India
[2]VTU, Belgaum, Karnataka, India
E-Mail: raja@nal.res.in

ABSTRACT

The surface bonded PZT transducers are employed to generate high frequency guided waves to detect damages in structural health monitoring and non-destructive evaluation schemes. These sensors' may undergo different operational loadings, which can cause damages to them. Hence, in the present work, a methodology is proposed to detect the sensor debonding using fundamental anti-symmetric Lamb wave mode. The PZT sensor when subjected to a propagating Lamb wave field, exhibits a unique maximum peak voltage, which depends on the sensor dimension and wavelength of the propagating Lamb wave. Sensor debonding changes the effective bonding surface, resulting in the shift of the peak voltage response in the frequency scale. Therefore, this shift in the frequency due to debond has been identified as a parameter to detect damage in the sensor. The procedure involves, computing the Maximum Amplitude Spectra (MAS) of each sensor and monitor the changes in peak amplitude and its corresponding frequency. Further, debonded sensor output is found to be reduced, which is also a parameter to assess the damage in the sensor. However, reduction in sensor output may also occur due to the presence of damage in structure; hence it is difficult to make damage prediction based on sensor voltage alone. It is noticed that the time of flight (TOF) between emitter and receivers (PZT sensors) is also affected by sensor debonding. Therefore, by monitoring MAS of each PZT sensor for a given frequency band of excitation and computing TOF, one can find the presence of damage in sensor and its integrity with respect to the host structure.

Keywords: debonding, lamb waves, non destructive evaluation, PZT sensors, sensor diagnosis, structural health monitoring.

INTRODUCTION

Structural Health Monitoring (SHM) is an emerging area, in which the health and condition of a system has been observed using an array of sensors and the collected data is periodically assessed for identifying the damage, if any. Different damage detection and monitoring methodologies are developed using mechanical/electrical/acoustical information, employing statistical method, signal proposing technique and probabilistic approaches etc. SHM has brought a new thrust to the design of aircraft/civil structures and mechanical systems by means of reducing their maintenance cost, besides improving safe operation and service life [1].

The occurrence of damage in a structure or mechanical system may change its material or geometric properties, which will affect the performance of the system. Therefore a periodical assessment of system states in time scale is very essential in order to evaluate the influence of damage on the health of the system [2].

SHM employs different kinds of sensors and piezoelectric materials are the prominent ones among them. The Lamb wave propagation can be initiated and the same is observed by using piezoelectric emitters and receivers, respectively. The Lamb wave with a frequency (wave length) can travel in thin plates that will capture the damage information along its travelling path/media. Thus Lamb wave acts as a carrier of the required damage related information in SHM application. There are two fundamental Lamb wave modes (A_0 and S_0) existing, which can be effectively generated through thin piezoelectric patches as emitters [1].

Ajay and Cesnik [3] and Su *et al*., [4] have presented a detailed survey of different works carried out on the application of guided Lamb waves in SHM. Victor [5] has explored the capability of embedded piezoelectric wafer active sensor (PWAS) to excite and detect tuned Lamb waves for SHM. There are two techniques which are popularly adopted for damage identification, namely pulse-echo and pitch-catch methods. Based on these techniques various literatures can be found for their application to identify damages in isotropic and composite structures such as holes, cracks, delamination using A_0/S_0 Lamb wave modes [6-17]. Sensor/actuator debonding alters the systems' response measurement, i.e. changes in amplitude, phase besides modifying their electrical capacitance / admittance. Hence, various attempts have been made by observing these changes to identify and quantify the extent of debonding in transducers [18-26]. Giulia *et al*., [18] have demonstrated the sensor debonding detection by observing the changes in amplitude and phase of the piezoelectric voltage response. Sang and Hoon [19] have proposed a PZT transducer self-diagnostic technique based on time-reversal process. They have included the effects of temperature and structural condition variations in their diagnostic technique.

Park *et al*., [20] have developed a self-diagnostic procedure for piezoelectric sensors by tracking the changes in their capacitance. Any degradation in capacitance alters the coupling capability of piezoelectric transducer with host structure. This is observed as changes

in the imaginary part of measured electrical admittance. Timothy *et al*., [21] have devised a procedure to detect sensor debonding by measuring the electrical admittance and its variation due to temperature is further examined. Gyuhae *et al*., [22] have proposed a sensor diagnostics procedure by measuring the electrical impedance of the sensor. Studies are also carried out to understand the effect of sensor debonding on the response measurement of the SHM system using Lamb wave / Impedance based methods. Seungee *et al*., [23] have developed impedance models that accommodate sensor debonding, where debond is identified by observing the changes in electrical admittance of the transducer. Hector and Alberto [24] have presented a unique technique of segmenting the sensor into three parts. To check debonding, the voltage responses are inter-compared and changes in the linearity of the signal output is identified as the presence of debond in the transducer. Further, the effect of thickness and the length of bonding layer on the electrical signature of piezoelectric sensor have been studied to identify the debonding [25]. Mohammad *et al*., [26] have carried out an assessment to quantify the degradation in electric and electromechanical characteristics of polymer composite PZT sensors, under fatigue loading.

Francesco *et al*., [27], Victor [28] and Ajay and Carlos [29] has studied the response of PZT sensors to ultrasonic waves, wherein response to Rayleigh waves and Lamb waves are examined. Researchers in SHM community have adopted different procedures to diagnose PZT sensors' debonding in the structure. The measured variables such as admittance measurement [20-22], impedance measurement [22-23], temperature effect on the sensors [22], reciprocity between time response of two PZT sensors and time reversal of the signals using Lamb waves [15], electrical properties of PZT sensors [24-25] and debonding based on maximum amplitude [18] have been studied to identify the sensor debonding/bonding related defects. Analytical and numerical studies [20-23, 27, 29] are performed to evaluate the effects of interface debonding on the performance of piezoelectric (PZT) sensor for Structural Health Monitoring systems.

In general, a completely broken sensor/actuator can be easily identified, if a sensor does not produce any measurable output, or an actuator does not respond to applied signals. However, if only a small fracture/debonding occurs within the materials, sensors/actuators are still able to produce sufficient performance with distorted signals potentially leading to a false indication of the structural condition. For piezoelectric sensors, the failures are inevitable after extreme natural hazards. The mechanical and electrical properties of PZT materials can gradually degrade over their service life. The degradation in sensor quality may bring false alarming and non-utilization of SHM system, if one needs to employ large numbers of sensors/actuators over a long period of time.

It is understood from the literature review that the transducer dimensions play an important role in determining the frequency at which the peak sensor response occurs. Also it can be noticed that, changes / degradation in the contact surface between transducer and host structure may effectively change the sensing dimension of the transducer. Therefore in the present work, the Maximum Amplitude Spectra has been computed for each sensor and used as a parameter to detect debond in a circular array of sensors, which are optimized sensory network in SHM system. Further for effective localization of damage occurrence in the PZT sensors, three types of damage models are introduced and their identification is evaluated through experiments.

SENSOR DAMAGE IN CIRCULAR ARRAY WITH LAMB WAVE TECHNIQUE

A critical aspect of the piezoelectric active technologies is that usually a large number of distributed sensors and actuators are needed to perform the required monitoring process. In addition, the structures in question are usually subjected to various external loadings and environmental conditions that may adversely affect the functionality of SHM sensors and actuators. Most current monitoring systems are not intelligent enough to differentiate signal changes, caused by damage from those due to sensor failures. The piezoelectric sensors/actuators self-diagnostic procedure, where they are confirmed to be operational, is therefore a critical component to successfully complete the SHM process. The importance of bond integrity between a PZT wafer and a host structure can be understood intuitively. The fundamental assumption in piezoelectric active-sensing technologies is that the sensors and actuators are perfectly bonded to a structure, and the integrity of the bonding layer does not change throughout their service lives, which is not the case in real-world applications. For instance, the adhesives used for bonding the PZT patch have a finite service life, usually shorter than the host structure's lifespan [20].

In the present work we propose a procedure to identify the sensor debonding using Lamb wave propagation technique in aluminum plates. The basis of this procedure is to generate the Maximum Amplitude Spectra (MAS) for each sensor response and monitor its variation in terms of amplitude and frequency of the propagating Lamb wave. Maximum Amplitude Spectra (MAS) is the frequency spectrum, generated from the peak values of the positive envelop of response signals to a range of excitation frequencies of the Lamb wave. The peak amplitude and its corresponding frequency from MAS for perfectly bonded sensors are considered as reference values for evaluating sensor debonding. On the other hand, the peak amplitude and its frequency of the debonded PZT sensor are observed with respect to the reference values. These variations in amplitude and frequency can be used to assess debonding in PZT sensors. Therefore, by monitoring the variation in amplitude and frequency, one can qualitatively examine the debonding in PZT sensor and its integrity with host structure. Time of flight (TOF) and group velocity (Vg) are marginally affected by sensor debonding. Hence these two parameters are used as additional parameters to identify the sensor

debonding. Further, three different types of sensor debonding cases are considered and evaluated.

METHODOLOGY

The schematic of the plate structure along with healthy and damaged sensors is shown in Figure-1. The PZT patches in a circular configuration have been surface mounted on top of a aluminum plate. These PZT patches are treated as receivers. Two more PZT patches are surface bonded, one on the top and other at the bottom of the plate. These PZT patches are used as emitters in order to generate either A_0 or S_0 Lamb wave. The Lamb wave with a desired frequency and number of cycles is generated using sine signal, windowed with standard Hanning window. A Matlab based program is developed to generate this Lamb wave and the generated waveform is fed to a function generator. This wave form is stored in a high end function generator and its frequency and amplitude can be modified as per the requirement. Lamb waves generated by the emitters are seen propagating in the plate structure in all directions. The distributed receivers on the plate structure are connected to a high impedance device i.e. storage oscilloscope to capture the propagating Lamb waves' signals. The required data is stored into the flash drive of the oscilloscope in standard ascii format. Data is then exported to a signal processing computer through USB port. The above procedure is repeated for different Lamb wave frequencies to identify the peak response and construct the maximum amplitude spectra for all the sensors.

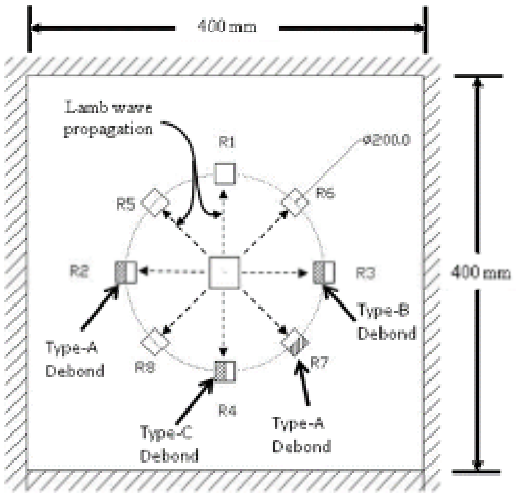

Figure-1. Array of circular sensors (healthy and damaged).

Three kinds of sensor debond have been considered in the present work, namely Type-A, Type-B and Type-C (see Figure-1). In Type-A debond, the propagating wave meets the bonded region first (approaching edge) and then continues to travel through the debonded region. Here the contact length of the sensor along the wave propagation is reduced due to debond. On the other hand in Type-B debond, the propagating wave meets the debonded region first and then followed by the bonded region. As in Type-A, the contact length of the sensor along wave direction is reduced due to debond. The propagating wave meets the bonded and debonded regions simultaneously and also the contact length along the wave propagation direction remains the same in Type-C debond.

The data from all the sensors and emitters are collected together to form a single file for a given excitation frequency. All the signals are purified using wavelet denoising algorithm and the positive envelop is estimated for each signal. The peak of the response and its time of occurrence are extracted from all the estimated envelops. For all the sensors, the MAS plots are generated from the extracted peak response values with respect to corresponding actuation frequencies. These MAS plots are then used to characterize the sensor debonding and type of sensor debonding. Time of flight (TOF) and group velocity (Vg) are calculated from these extracted parameters.

THEORETICAL FORMULATION

There are two major kinds of waves in solid media-guided waves and bulk waves [30, 31]. Bulk waves travel in the bulk of the material, hence away from the boundaries. In contrast, the solution to a guided wave problem must satisfy the governing equations as well as some physical boundary conditions. Unlike the finite number of modes that might be present in a bulk wave problem, there are generally an infinite number of modes associated with a given guided wave problem. For plates, the propagation conditions have been described by Lamb and the waves are known as Lamb waves. They are waves of plane strain that occur in a free plate, and the traction force must vanish on the upper and lower surface of the plate.

The solution to the free plate problem can be derived from the following equations:

$$\frac{\tan(qh)}{\tan(ph)} = -\frac{4k^2pq}{(q^2-k^2)^2} \quad \text{for symmetric modes} \qquad (1)$$

$$\frac{\tan(qh)}{\tan(ph)} = -\frac{(q^2-k^2)^2}{4k^2pq} \quad \text{for antisymmetric modes} \qquad (2)$$

where $\left(p^2 = \omega^2/c_L^2\right) - k^2$ and $\left(q^2 = \omega^2/c_T^2\right) - k^2$, c_L is the longitudinal wave velocity, c_T is the shear wave velocity, k is the wave number, and h is half the thickness of the plate.

For the symmetric modes, the wave structure across the thickness of the plate is symmetric to displacement u and antisymmetric to angular frequency ω ; while for antisymmetric modes, the wave structure across the thickness is symmetric to ω and hence antisymmetric to u .

Equations (1) and (2) can be used to determine the velocity at which a wave of a particular frequency (fh or fd product, where f is frequency, d is the thickness of the plate) will propagate within the plate. Equations of this nature are known as dispersion relations. Although the equations look simple, they can be solved only by numerical methods.

When plotting the dispersion curves, the interest is to find the real solutions of these equations, which represent the (undamped) propagating modes of the structure. It is therefore useful to rewrite the above two equations so that they take on only real values for real or pure imaginary wave numbers k . This is achieved by the following set of eqations:

$$\frac{\tan(qh)}{q} + \frac{4k^2 p \tan(ph)}{([q^2 - k^2)]^2} = 0 \quad \text{for symmetric modes} \qquad (3)$$

$$q \tan(qh) + \frac{([q^2 - k^2)]^2 \tan(ph)}{4k^2 p} = 0 \quad \text{for antisymmetric modes} \qquad (4)$$

The wave number k takes on the value $k = 2\pi/\lambda = \omega/c_p$, where $\omega = 2\pi f$ and the phase velocity $c_p = f\lambda$, λ is the wavelength.

Group velocity is associated with the propagation velocity of a group of waves of similar frequency, also termed as 'velocity of wave packets'. After the phase velocity is determined numerically, the group velocity c_g can be found from the phase velocity c_p by using the formula $c_g = d\omega/dk$. Substituting k and ω, the equations become:

$$c_g = c_p^2 \left[c_p - (fd) \frac{dc_p}{d(fd)} \right]^{-1} \qquad (5)$$

where fd denotes frequency times thickness [32].

Analytically generated phase velocity and group velocity plots of symmetric and anti-symmetric Lamb wave modes for 1.5 mm thick aluminum plate are shown in Figures 2 and 3.

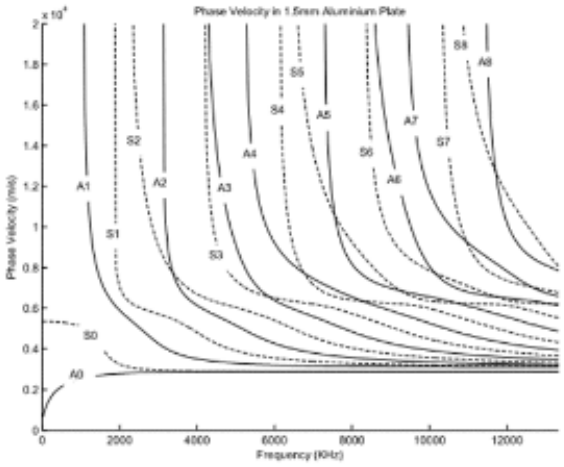

Figure-2. Phase velocities of Lamb wave mode.

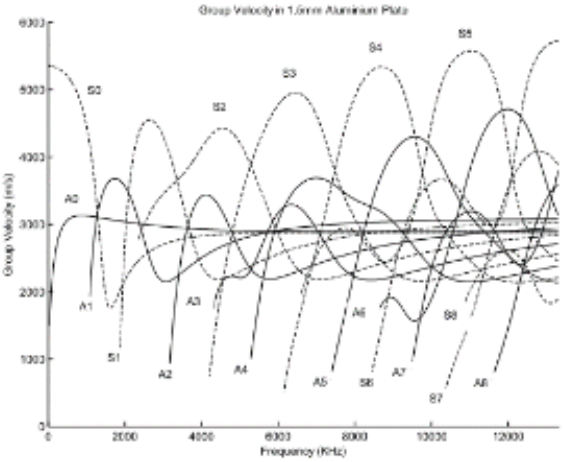

Figure-3. Group velocities of Lamb wave mode.

Dispersion curves for anti symmetric (A_0) and symmetric (S_0) Lamb wave modes for the plate considered in a frequency range of 1 to 100 kHz are shown in Figures 4 and 5.

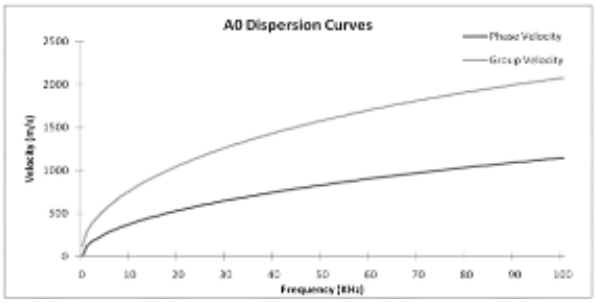

Figure-4. Dispersion curves of A_0 Lamb wave.

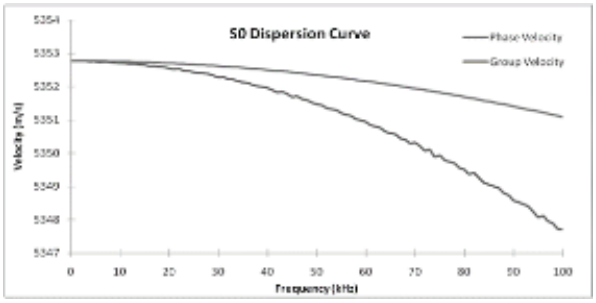

Figure-5. Dispersion curves of S_0 Lamb wave.

EFFECT OF SENSOR DEBONDING ON LAMB WAVE PROPAGATION

In order to assess the PZT sensor debonding, Lamb wave experiments are conducted on an aluminum plate structure, which is a representative of aircraft fuselage panel. The mechanical properties of this aluminum plate are given in Table-1.

Table-1. Mechanical properties of aluminum plate.

Young's Modulus (GPa)	72
Mass density (kg/m^3)	2700
Poisson's ratio	0.3

Two aluminum plates having dimensions of 500x500x1.5 mm^3 are instrumented with eight PZT sensors. These sensors are bonded in a circular array arrangement on a pitch circle diameter (PCD) of 200 mm such that the midpoints of the sensors get aligned to PCD. All the PZT sensors are perfectly bonded on one of the aluminum plates (Plate 1), whereas on the other aluminum plate (Plate 2) four PZT sensors are partially debonded. The dimensions of the PZT sensors are 10X10X0.5 mm^3. The PZT sensors are surface bonded using a standard epoxy adhesive (Araldite) and allowed it for curing as per standard guidelines. In order to simulate the damage in the PZT sensors, 50% of the PZT area is surface bonded using araldite and remaining area is not bonded. The PZT sensors are debonded in three ways i.e. type-A, type-B and type-C. In type-A and type-B 50% of the sensor length is debonded. In type-A the sensor is debonded outside the PCD whereas in type-B the sensor is debonded inside the PCD. In type-C, 50% of the sensor width is debonded. Two more PZT patches having dimensions of 15x15x0.5 mm^3 are perfectly bonded on top and bottom of the plates at the center and these PZT patches are used as emitters. The top and bottom emitters are designated as E1 and E2 and the eight receivers are marked as R1 to R8. The schematic of the instrumented plates is shown in Figure-6. The emitter PZT patches and sensor PZT patches are SP-5H type, supplied by M/s Sparkler Ceramics Pvt. Ltd., Pune, India and the properties of PZT patches are given in Table-2.

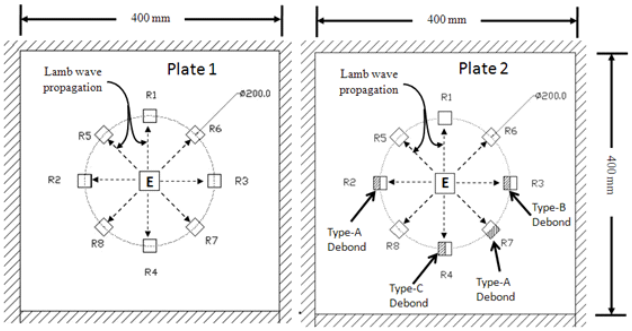

Figure-6. Schematic of instrumented aluminum plates.

Table-2. Properties of PZT patch.

Type	Dimensions (mm^3)	Capacitance (ηF)	d_{33} (pC/N)	K^T_3
SP-5H	15x15x0.5	10.0	585	3028
SP-5H	10x10x0.5	4.9	584	3168

EXPERIMENTAL SETUP

The instrumented plates are mounted independently on the fixture to simulate C-C-C-C boundary condition. The plate is placed in between two frames and mounted on the fixture using M6 bolts. All the bolts are tightened with proper torque using torque wrench in order to simulate the desired boundary condition. Experiments on the aluminum plate structure are conducted using Tektrononix Make dual channel arbitrary function generator and digital storage oscilloscope. The function generator (AFG30222B) is capable of generating signals up to 25 MHz with a maximum sampling rate of 250 MS/s. The storage oscilloscope (TDS2014B) is capable of acquiring signals up to 100 MHz with a sampling rate of 1 GS/s. The emitters are connected to the dual channel arbitrary function generator in order to generate desired Lamb waves in the aluminum plate structure. The receiving sensors are connected to high impedance device i.e. digital storage oscilloscopes to capture the propagating Lamb wave. The detailed experimental setup is shown in Figure-7.

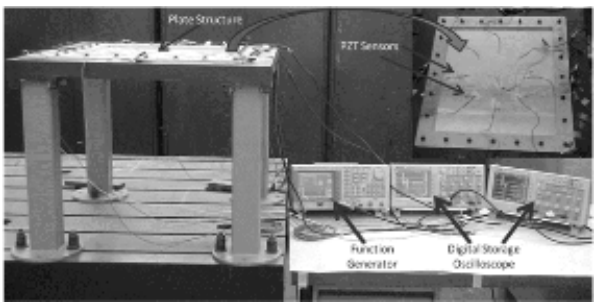

Figure-7. Experimental test setup.

The actuation pulse is generated in Matlab® for a desired frequency, number of cycles and these signals are

windowed with standard Hanning window. The generated pulse is fed to the function generator and stored in its memory. The actuation signal from function generator is fed to the emitters to generate the required Lamb wave. Actuation signals with 3, 3.5, 5 and 5.5 cycle pluses are considered to study the effectiveness of number of cycles on the response of receiving sensors. The responses plotted in Figure-8 indicates that the actuation signal with 3.5 cycles pulse gives better response compare to other actuation pulses. Based on this a 3.5 cycle windowed sine pulse actuation signal is considered throughout the experiments. In general, the basic anti-symmetric mode (A_0) and symmetric mode (S_0) are used for damage detection in thin structures. The dispersion curves (Figure-2 and 3) indicate that the fundamental A_0 and S_0 wave modes are appeared within the frequency range of 100 kHz for the structure under consideration. The A_0 Lamb wave is generated in the plate by actuating the top and bottom emitters in out-of-phase mode. Similarly, the S_0 Lamb wave can be generated in the plate by actuating the top and bottom emitters in in-phase mode. The other parameters considered are 20 V_{p-p} actuation voltage, one pulse of Lamb wave consists of 3.5 cycle windowed sine signal, time delay of 3sec between two successive pulses. The actuation pulse frequency is swept from 10 to 100 kHz in steps of 10 kHz. The sensor responses are sampled at 5 MHz with 16 linear averages and the raw data is stored in flash memory.

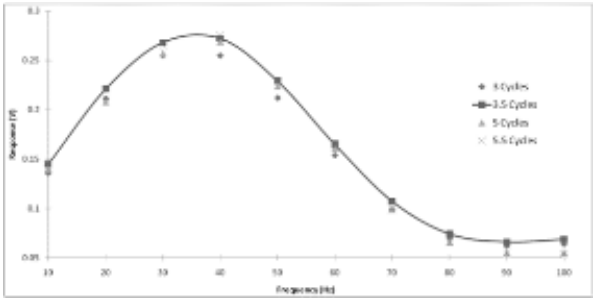

Figure-8. Response for different number of cycle.

Experimentally calculated group velocity of the Lamb wave between emitter and receivers for plate 1 are compared with analytically estimated values and they are presented in Figure-9. A good correlation exists between analytically calculated and experimentally measured group velocity for plate 1, which shows that Lamb waves of desired frequency are accurately generated by the emitters and also captured by the receivers (PZT).

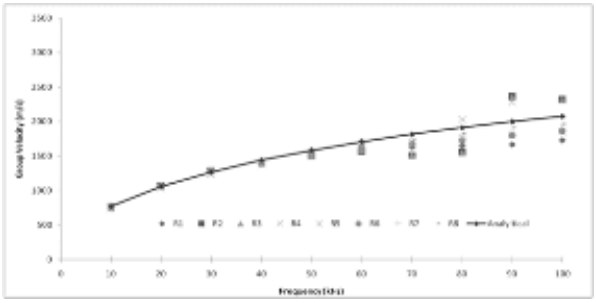

Figure-9. Group velocity of Lamb wave (Plate-1 sensors).

ANALYSIS

The individual sensor responses for each actuation frequency are collected to a single file for better handling and visualization of data. The responses are processed using Time-frequency analysis module of DATS® software. The time responses are denoised using wavelet denoising algorithm with parameters such as Morlet type of wavelet, 1/32 octave spacing and parabolic mode. The positive time varying envelop is computed using Fourier transform technique for all the denoised responses.

The Peak of the response and its time of occurrence are extracted from all the estimated envelops. From these parameters, Time-of-flight (TOF) is calculated. TOF is the time taken by the pulse to travel from emitter to receiver. Also, group velocity of the propagating Lamb wave for all the receiver locations is calculated. The group velocity (V_g) is the ratio between distance travelled (emitter to receiver) by the pulse to its corresponding TOF. The Maximum Amplitude Spectra (MAS) for each sensor is generated using peak amplitude from envelop and its corresponding actuation signal frequency. The typical MAS for sensor R1 of plate 1 is shown in Figure-10.

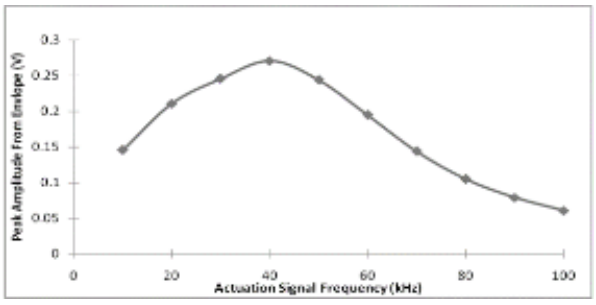

Figure-10. Typical MAS for sensor R1 of Plate-1.

RESULTS AND DISCUSSIONS

Maximum amplitude spectrum for all the sensors of plate 1 and plate 2 for the excitation frequency band of 10 to 100 kHz in steps of 10 kHz is estimated and they are plotted in Figure-11 and Figure-12.

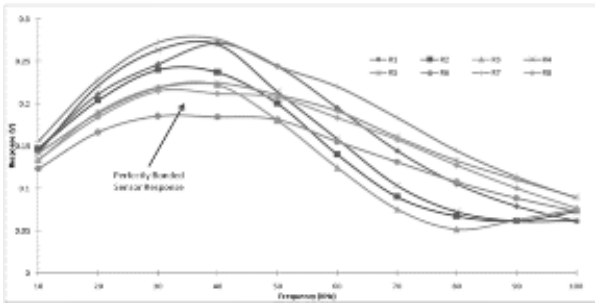

Figure-11. Sensors response of Plate-1.

The MAS of all the perfectly bonded sensors indicates that the peak amplitude occurs at a constant frequency of 35 kHz and maximum response spectra of all the sensors shows the similar trend as expected.

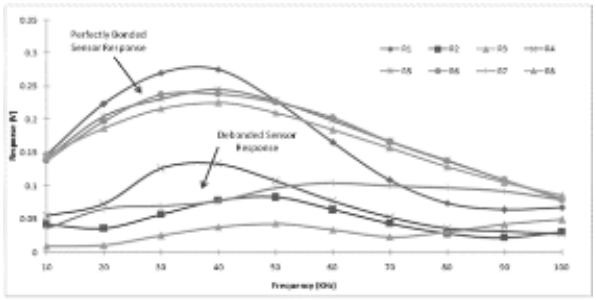

Figure-12. Sensors response of Plate-2.

The responses from the type A and B debonded sensors indicate that the peak amplitude response reduces and frequency shifts from 35 kHz to 50 kHz. For type C debonding the peak response is reduced to 50% without change in peak response frequency and the overall trend remains same as perfectly bonded sensors. The variation in amplitude and frequency of MAS clearly indicates debonding in the sensors and its type.

TOF is affected by the sensor debonding and these changes have reflected on the group velocity (Vg). The TOF values for different sensors (R2 R3 and R4) from plate 1 and Plate 2 are shown in Figure-13. These results indicate a small variation in TOF of sensors R2 (type-A) and R4 (type-C) between plate 1 and plate 2. This is due to debonding introduced outside the PCD in case of sensor R2; along width wise in case of sensor R4. Variation in TOF of sensor R3 (type-B) between plate 1 and plate 2 is more, compare to sensors R2 and R4 due to presence of debonding inside PCD.

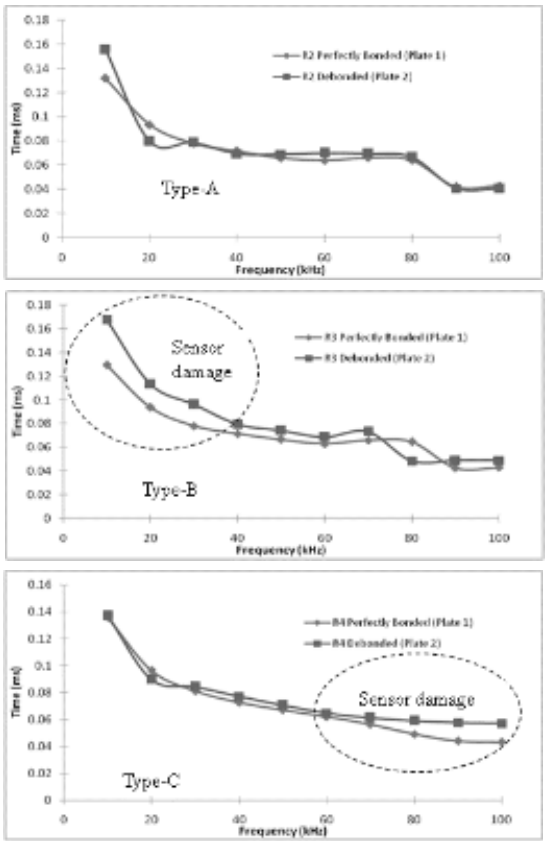

Figure-13. Variation of TOF between perfectly bonded and debonded sensors.

Based on the experimental results, the following major observations are made.

- When damage occurs in a sensor, predominately creating debonding across the direction of the Lamb wave propagation, it is observed that the peak amplitude of the MAS shifts towards the higher frequency.
- On contrast, when damage takes place in a sensor that induces debonding along the direction of wave propagation, it is noticed that only amplitude reduction happens without any significant frequency shift.
- In the group velocity calculation one can see that for a given sensor size the simulation and experiment matches well. This must be considered as a design variable in SHM system. Also the size of the sensor brings limitation on the sensor effectiveness in receiving wider frequency band.
- In case of debonded sensors the deviation in group velocity noticed to be moderate in the complete operational frequency band.
- In Type-A debond, TOF does not provide any specific trend about the sensor damage.
- However, the TOF indicates the presence of damage when it occurs between approaching edge and pitch circle diameter (PCD), which is evident, through

identifying Type-B debonding (before the peak response frequency).

- If the debond occurs partially along the Lamb wave propagation (Type-C), the TOF reflects the presence of sensor damage after the peak response.

CONCLUSIONS

A novel methodology is demonstrated to assess the sensor debonding using Lamb wave by conducting experiments on aluminum plates. Three different types of sensor debonding are simulated and evaluated using the proposed procedure. Peak response of the sensors and frequency shift in the maximum amplitude spectra are used as parameters to assess the sensor debonding. Lamb waves are generated experimentally using two surface mounted PZT patches. Also, PZT transducers are employed as sensors for capturing the transmitted Lamb waves through the plate structure. Analytically estimated group velocities of A_0 Lamb wave are validated with the experimentally calculated values. The sensor debonding characteristics are well established from the time response signals using positive envelop method and maximum amplitude spectra. The type-A and type-B debonding show reduction in amplitude and increase in frequency whereas, the type-C debonding shows reduction in amplitude but no variation in its corresponding frequency. Using the proposed methodology, sensor debonding can be qualitatively examined in-situ and the technique can be used in SHM applications.

ACKNOWLEDGEMENTS

The authors gratefully thank Mr. S. Vedaprakash and Mr. M. Mahesh, Scientific Assistants for their help rendered in instrumenting the specimens. The financial assistance received to carry out this research work as a part of SIP-STTD-06 project (Development of damage tolerant smart structures) under CSIR-NAL 11th FYP has been acknowledged.

REFERENCES

[1] Steven R. Anton, Adam Butland, Migdalia Carrion, Miles Buechler and Gyuhae Park. 2007. Instantaneous Structural Damage Identification Using Piezoeletric - Based Lamb Wave Propagation. IMAC XXV, SEM.

[2] Inman D.J., Farrar C.R., Lopes Jr. and Valder Jr. 2005. Damage Prognosis for Aerospace, Civil and Mechanical Systems. John Wiley and Sons, Ltd., West Sussex, England.

[3] Ajay Raghavan and Carlos E.S. Cesnik. 2007. Review of Guided-wave Structural Health Monitoring. The Shock and Vibration Digest. 39(2): 91-114.

[4] Zhongqing Su, Lin Ye and Ye Lu. 2006. Guided Lamb waves for identification of damage in composite structures: A review. J. of Sound and Vibration. 295: 753-780.

[5] Victor Giurgiutiu. 2011. Piezoelectric wafer active sensors for structural health monitoring of composite structures using tuned guided waves. J. of Engineering Materials and Technology. 133: 041012-1

[6] Chul Min Yeum, Hoon Sohn, Jeong Beom Ihn and Hyung Jin Lim. 2012. Instantaneous delamination detection in a composite plate using a dual piezoelectric transducer network. Composite Structures. 94: 3490-3499.

[7] Dong Wang, Lin Ye, Zhongqing Su and Ye Lu. 2011. Quantitative identification of multiple damage in laminated composite beams using A0 Lamb mode. J. of Composite Materials. 45(20): 2061-2069.

[8] Hong Yue Tang, Charles Winkelmann, Wahyu Lestari and Valeria La Saponara. 2011. Composite structural health monitoring through use of embedded PZT sensors. J. of Intelligent Material Systems and Structures. 22: 739-755.

[9] N. Hu, Y. Liu, X. Peng and B. Yan. 2010. Optimal excitation frequency of Lamb waves for delamination detection in CFRP laminates. J. of Composite Materials. 44(13): 1643-1663.

[10] Victor Giurgiutiu. 2011. Piezoelectric wafer active sensors for structural health monitoring of composite structures using tuned guided waves. J. of Engineering Materials and Technology. 133: 041012-1.

[11] Jeong Beom Ihn and Fu Kuo Chang. 2008. Pitch-catch active sensing methods in structural health monitoring for aircraft structures. Structural Health Monitoring. 7(1): 5-19.

[12] Ning Hu, Takahito Shimomukai, Hisao Fukunaga and Zhongqing Su. 2008. Damage identification of metallic structures using A0 mode of Lamb waves. Structural Health Monitoring. 7(3): 271-285.

[13] Wahyu Lestari and Pizhong Qiao. 2005. Application of wave propagation analysis for damage identification in composite laminated beams. J. of Composite Materials. 39(22): 1967-1984.

[14] Victor Giurgiutiu. 2005. Tuned Lamb wave excitation and detection with piezoelectric wafer active sensors for structural health monitoring. J. of Intelligent Material Systems and Structures. 16: 291-304.

[15] Banibrata Poddar, Christudas R Bijudas, Mira Mitra and Prasanna M Mujumdar. 2012. Damage detection in a woven-fabric composite laminate using time-reversed Lamb wave. Structural Health Monitoring. 11(5): 602-612.

[16] Sauvik Banerjee, Fabrizio Ricci, Ernesto Monaco and Ajit Mal. 2009. A wave propagation and vibration-based approach for damage identification in structural components. J. of Sound and Vibration. 322: 167-183.

[17] N. Chakraborty, V.T. Rathod, D. Roy Mahapatra and S. Gopalkrishnan. 2012. Guided wave based detection of damage in honeycomb core sandwich structures. NDT and E International. 49: 27-33.

[18] Giulia Lanzara, Youngki Yoon, Yujun Kim and Fu-Kuo Chang. 2009. Influence of Interface Degradation on the Performance of Piezoelectric Actuators. J. of Intelligent Material Systems and Structures. 20: 1699-1710.

[19] Sang Jun Lee, Hoon Sohn, Jennifer E. Michaels and Thomas E. Michaels. 2010. In: Situ Detection of Surface-Mounted PZT Transducer Defects Using Linear Reciprocity. Review of Quantitative Nondestructive Evaluation. 29: 1844-1851.

[20] Park G., Farrar C.R., Rutherford C.A. and Robertson A.N. 2006. Piezoelectric Active Sensor Self-Diagnostics Using Electrical Admittance Measurements. ASME Journal of Vibration and Acoustics. 128: 469-476.

[21] Timothy G. Overly, Gyuhae Park, Kevin M. Farinholt and Charles R. Farrar. 2008. Piezoelectric Active-Sensor Diagnostics and Validation using Instantaneous Baseline Data. LA-UR-08-03082.

[22] Gyuhae Park, Charles R. Farrar, Francesco Lanza di Scalea and Stefano Coccia. 2006. Performance Assessment and Validation of Piezoelectric Active-Sensors in Structural Health Monitoring. Smart Materials and Structures. 15(6): 1673-1683.

[23] Seungee Park, Gyuhae Park, Chung-Bang Yun and Charles R. Farrar. 2009. Sensor Self-diagnosis Using a Modified Impedence Model for Active Sensing-based Structural Health Monitoring. Structural Health Monitoring. 8(1): 71-82.

[24] Hector A. Tinoco and Alberto L. Serpa. 2012. Voltage relations for debonding detection of piezoelectric sensors with segmented electrode. Mechanical Systems and Signal Processing. 31: 258-267.

[25] Hector A. Tinoco, Alberto L. Serpa and Angel M. Ramos. 2010. Numerical study of the effects of bonding layer properties on electrical signatures of piezoelectric sensors. Mecanica Computacional. 29: 8391-8409.

[26] Mohammad Mehdizadeh, Sabu John, Chun H Wang, Viktor Verijenko and Paul Callus. 2012. Delineation of Structural Damage from Piezo-Fibre-Based Sensor Degradation. International Journal of Engineering Science and Technology. 4(01): 247-264.

[27] Francesco Lanza di Scalea, Howard Matt and Ivan Bartoli. 2007. The response of rectangular piezoelectric sensors to Ralyleigh and Lamb ultrasonic waves. J. of Acoustical Society of America. 121(1): 175-187.

[28] Victor Giurgiutiu. 2002. Lamb Wave Generation with Piezoelectric Wafer Active Sensors for Structural Health Monitoring. SPIE's 10th Annual Intl. Symposium on Smart Structures and Materials & 8th Annual Intl. Symposium on NDE for Health Monitoring and Diagnostics, Paper # 5056-17.

[29] Ajay Raghavan and Carlos E.S. Cesnik. 2005. Finite-dimensional piezoelectric transducer modeling for guided wave based structural health monitoring. Smart Materials and Structures. 14: 1448-1461.

[30] Viktorov I.A. 1967. Rayleigh and Lamb Waves - Physical Theory and Applications. Plenum Press, New York, USA.

[31] Rose J.L. 1999. Ultrasonic Waves in Solid Media. Cambridge University Press, Cambridge, United Kingdom.

[32] Hua Gu and Ming L. Wang. 2009. A monolithic Interdigitated PVDF Transducer for Lamb Wave Inspection. Structural Health Monitoring. 8(2): 137-148.